# Reconfigurable Intelligent Surface Deployment and Orientation in Beyond 5G Multicast Networks

**Conference Paper** · June 2023

DOI: 10.1109/BMSB58369.2023.10211255

# Reconfigurable Intelligent Surface Deployment and Orientation in Beyond 5G Multicast Networks

Gianluca Brancati*, Ernesto Fontes Pupo‡, Olga Chukhno*,†, Nadezhda Chukhno†,
Maurizio Murroni‡, and Giuseppe Araniti*
*University Mediterranea of Reggio Calabria, Italy and CNIT, Italy
†Tampere University, Finland
‡University of Cagliari, Italy
e-mail: {*gianluca.brancati, olga.chukhno, araniti*}*@unirc.it, e.fontespupo@studenti.unica.it,*
*nadezda.chukhno@tuni.fi, murroni@diee.unica.it*

***Abstract*—As 5G evolves into a unifying connectivity fabric, new capabilities will emerge, enabling and enhancing such services as extended reality (XR), holographic telepresence, and other high-speed immersive experience. These multimedia applications demand strict latency, improved network capacity and coverage, and mobility support. Multicast transmissions, highly directional communications, and reconfigurable intelligent surfaces (RISs), combined with artificial intelligence, are expected to ensure such requirements. We present and solve the optimal RIS deployment and orientation problem for cellular highly-directional multicast connectivity based on the multilevel facility location model. We then develop and test two artificial intelligence alternatives, which offer a close-to-optimal solution with lower computational complexity. Our numerical results demonstrate that optimally deploying RISs enhances the average network throughput and latency of directional multicasting.**

***Index Terms*—5G NR, beyond 5G, multicasting, cellular networks, network planning, reconfigurable intelligent surfaces, machine learning.**

## I. Introduction

The envisaged fifth generation (5G) New Radio (NR) and beyond (B5G) mobile broadband communication offers unprecedented breakthroughs in media service delivery [1]. As 5G and B5G evolve into a unifying connectivity fabric, new capabilities will emerge, enabling and enhancing disruptive services such as extended reality (XR), holographic telepresence, and other high-speed immersive experience. Such multimedia applications demand strict latency, improved network capacity, coverage, and mobility support for a potentially high number of concurrent users.

In such a challenging context, the multicast/broadcast capability provides cost-effective and resource-efficient delivery mechanisms to multiple end-users requesting the same contents [2], [3]. Tailored point-to-multipoint communication strategies can provide considerable capacity gain into the B5G ecosystem for massive Internet of things (IoT) deployments, vehicular communications, and future multimedia applications. The 3rd Generation Partnership Project (3GPP) is working on the novel multicast and broadcast services (MBS) for the overall next-generation radio access network (NG-RAN) and 5G core network (5GC) perspectives [2].

Multicasting has traditionally been associated with omnidirectional communication at sub-6 GHz frequency bands [4]. In the last years, multicasting has gained momentum in highly directional millimeter wave (mmWave) and terahertz (THz) communications with massive multiple-input-multiple-output (MIMO) [5], which bring new challenges related to high propagation loss, severe signal attenuation due to blockage (e.g., human blockage of 15 dB), and reduced coverage [6]. The ineffective handling of these impairments can considerably reduce the multicast group's quality of service (QoS).

Lately, a novel technological breakthrough, named reconfigurable intelligent surfaces (RIS), has been proposed to enrich the scattering environment by enabling strong reflective signal paths between the base station (BS) and end-users [7]. As defined in [8], RIS is a planar surface comprising many low-cost passive reflecting elements, able to induce an amplitude and/or phase change to the incident signal independently. Therefore, RIS-aided mmWave multicasting can reduce the severe blockage effects in efficient resource management and the corresponding QoS. Moreover, RISs can improve network coverage without the deployment of numerous low-power BSs leading to a cost reduction [9]. However, RIS has several open research challenges yet to be addressed in its development and implementation.

In [10], multicast video services aided by RIS technology are investigated in high-traffic areas to optimize the 5G wireless transmission link and increase overall system capacity. The proposal is validated at sub-6 GHz bands, which do not capture the effect of propagation and blockage associated with the mmWave. In [11], a capacity characterization for RIS-assisted multiple-antenna multicasting is proposed. The proposed approach considers a single RIS in a fixed location, letting open the critical challenge of optimizing the RIS deployment based on multicast users' distribution and optimal RIS orientation.

The deployment of RIS is a critical challenge that needs to be addressed to fully leverage the benefits of highly directional communication. In [12] and [13], the RIS deployment problem

This is the post-print of the following article: Brancati, G., Pupo, E.F., Chukhno, O., Chukhno, N., Murroni, M. and Araniti, G., 2023, June. Reconfigurable Intelligent Surface Deployment and Orientation in Beyond 5G Multicast Networks. Article has been published in final form at: https://ieeexplore.ieee.org/abstract/document/10211255.
DOI: 10.1109/BMSB58369.2023.10211255 

has been formalized and solved for unicast applications aided by aerial-RIS scenarios and a relay system, respectively. These proposals do not consider classic terrestrial scenarios, multicasting capability, or RIS orientation. As a result, optimal RIS deployment and orientation for use cases with multiple users requesting the same multicast content over highly directional channels in the mmWave frequency band has not been sufficiently examined.

To bring this gap, this work addresses the RIS deployment and orientation problem for B5G highly-directional multicast connectivity. We present the optimal RIS deployment and orientation based on a multilevel facility location problem formulation. We then develop and test artificial intelligent alternatives to offer a close-to-optimal solution to the RIS deployment and horizontal orientation problem. The proposed frameworks are examined through system-level simulations, with a particular emphasis on network throughput, latency, and accuracy of machine learning (ML) algorithms.

The rest of this paper is organized as follows. Section II illustrates our system model. Section III describes the RIS deployment framework and the proposed supervised ML algorithms. In Section IV, the numerical results and corresponding analysis are presented. Finally, the conclusions are drawn in Section V.

## II. System Model

This section outlines a representative RIS-assisted multicast system illustrated in Fig. 1 and summarizes our modeling assumptions on the deployment, antenna, propagation, and blockage models.

We consider a 5G NR/B5G cellular outdoor deployment where $N_{\text{UE}}$ user equipment (UE) devices from set $\mathcal{N}_{\text{UE}} = \{1, ..., N_{\text{UE}}\}$ are scattered about the plane according to some independent homogeneous point process. An NR BS transmits multimedia data to $N_{\text{UE}}$ UEs utilizing directional mmWave multicast transmissions operating at the central frequency of $f_c = 28\,\text{GHz}$.

The NR BS is equipped with planar antenna arrays with radiation patterns similar to a conical space. The antenna gain can be calculated as follows [14]:

$$G_{tx} = D_0 \rho(\alpha), \tag{1}$$

where $D_0$ represents the maximum directivity along the antenna boresight and $\rho(\alpha) \in [0; 1]$ is a linear function scaling the directivity $D_0$. We note that $\rho(\alpha)$ depends on the angular deviation of the transmit/receive direction from the antenna boresight $\alpha$, whereas $D_0$ depends on the number of antenna elements $N_{\text{AE}}$.

We consider an urban scenario and characterize the propagation pattern according to the 3GPP urban microcell (UMi) Street Canyon path loss model [15]. UEs can also experience blockage by small- and large-scale objects. Specifically, *NLoS state* describes blockage by a large static object (e.g., buildings and permanent structures), while a *blocked state* with 15 dB attenuation occurs when the path between the BS and a UE (or a multicast group) is obstructed by a human body

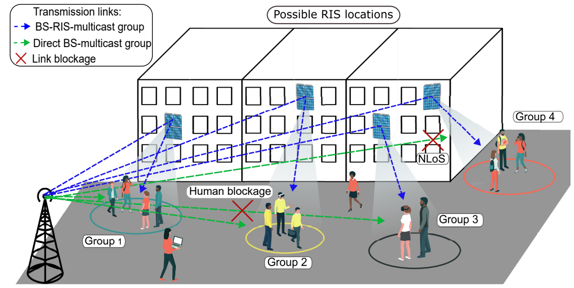


Fig. 1. Illustration of considered RIS-assisted multicast system.

and foliage [16]. Therefore, the following four states are experienced by multicast group users: *(i)* LoS non-blocked, *(ii)* LoS blocked, *(iii)* NLoS non-blocked, and *(iv)* NLoS blocked states.

The associated UMi path loss measured in dB is given by:

$$L_{dB}(y) = \beta + 10\zeta \log_{10} y + 20 \log_{10} f_c, \tag{2}$$

where $f_c$ is the carrier frequency in GHz, $y$ is the three-dimensional (3D) distance between the BS and the UE in m, whereas $\beta$ and $\zeta$ are the blockage and propagation coefficients, respectively. Namely, $\zeta = 2.1$ and $\zeta = 3.19$ correspond to LoS and NLoS states, whereas $\beta = 32.4$ and $\beta = 47.4$ represent non-blocked and blocked states. The linear scale representation of (2) is written as: $L(y) = (10^{2\log_{10} f_c + \frac{\beta}{10}}) y^{\zeta}$.

The total received power $P_{rx}$ at the UE is calculated as

$$P_{rx} = P_{tx} G_{tx} G_{rx} L^{-1}(y) = \frac{P_{tx} G_{tx} G_{rx}}{L(y)}, \tag{3}$$

where $G_{tx}$ is the transmit antenna gain, $G_{rx}$ is the receive antenna gain, and $L(y)$ is the linear path loss. We recall that the UE with the worst channel conditions defines the channel conditions of the multicast group.

The LoS probability may be defined as in [15]:

$$p_L(x) = \begin{cases} 1, & x \leq 18\text{m}, \\ 18 + x e^{-\frac{x}{36}} - 18 e^{-\frac{x}{36}}, & x > 18\text{m}, \end{cases} \tag{4}$$

where $x$ is the two-dimensional (2D) distance between the BS and a multicast UE.

The human blockage probability $p_B$ at distance $x$ can be calculated as provided in [17]:

$$p_{\text{B}}(x) = 1 - e^{-2\lambda_{\text{B}} r_{\text{B}} \left[x \frac{h_{\text{B}} - h_{\text{UE}}}{h_{\text{BS}} - h_{\text{UE}}} + r_{\text{B}}\right]}, \tag{5}$$

where $\lambda_{\text{B}}$ is the blocker density, $h_{\text{B}}$ and $r_{\text{B}}$ are the blocker height and radius, $h_{\text{BS}}$ is the BS height, and $h_{\text{UE}}$ is the UE height, $h_{\text{B}} \geq h_{\text{UE}}$.

BS-RIS-multicast group links may enhance direct BS-multicast group transmissions by improving the channel conditions on the worst multicast UE in the group. Therefore, we assume that RISs with $M_{\text{SE}} \times N_{\text{SE}}$ reflective elements of $s_{M_{\text{SE}}} \times s_{N_{\text{SE}}}$ size are deployed in the area of interest [18].

We consider RIS operating in the far-field region, then the distances between different RIS elements and the BS may be approximated as the distance between the BS (or source) and the center of the RIS, $d_{\text{SR}}$, i.e., $D_{m,n} \approx d_{\text{SR}}$. By analogy, the distance between RIS elements and a multicast group may be approximated as the distance between the RIS center and the multicast group (RIS-Destination), i.e., $d_{m,n} \approx d_{\text{RD}}$.

The total received power at the multicast UE through the RIS can be obtained as in [19]:

$$P_{rx} = \left( \sum_{q} \sqrt{\frac{P_{tx} |\Gamma_q| G_{tx} G_{rx}}{L(d_{\text{SR}}) L(d_{\text{RD}})}} e^{j\phi_q} \right)^2, \tag{6}$$

where $L(d_{\text{SR}})$ is the BS-RIS path loss, $L(d_{\text{RD}})$ is the RIS-multicast UE path loss, $\phi_q$ represents the phase delay of the signal received through the $q$-th reflective element, and $\Gamma_q$ is the $q$-th reflective element reflection coefficient calculated as:

$$\Gamma_q = e^{-j\varphi_q G_i^e G_r^e \epsilon_b}, \tag{7}$$

where $\varphi_q$ is the phase difference induced by the $q$-th reflective element, $G_i^e$ is the RIS gain in the incoming wave direction, $G_r^e$ is the RIS gain in the received wave direction, and $\epsilon_b$ is the RIS element efficiency, which can be expressed as the ratio of transmit signal power emitted by the RIS to the received signal power by the RIS.

The data rate of a RIS-enhanced link can be calculated employing the Shannon-Hartely theorem:

$$D[\text{Gbps}] = W \times 10^{-9} \log_2 \left( 1 + \frac{P_{rx}}{N_0 W} \right), \tag{8}$$

where $W$ is the operating bandwidth in Hz, and $N_0$ is the power spectral density of noise.

## III. Proposed Framework

This section describes the proposed optimal RIS deployment framework and the setup of the employed ML algorithms to deal with the complexity of the optimal solution.

### A. Optimal RIS Deployment

We consider a set of multicast groups $\mathcal{N}_{\text{group}} = \{1, \ldots, N_{\text{group}}\}$. We assume that RISs can be deployed in a set of candidate sites, $\mathcal{L}_{\text{RIS}} = \{1, \ldots, L_{\text{RIS}}\}$ and with a fixed orientation, $\mathcal{L}_{\theta} = \{1, \ldots, L_{\theta}\}$. Moreover, we define a set of possible locations for the BSs as $\mathcal{L}_{\text{BS}} = \{1, \ldots, L_{\text{BS}}\}$. The data rate experienced by the $i$-th multicast group served by the RIS located at node $j$ with orientation $l$ and BS placed at site $k$, $D_{ijkl}$, is obtained as per (8).

To formulate the optimal RIS deployment problem in B5G cellular multicast networks, we define a binary indicator $u_{ijkl}$ to denote RIS and BS assignment for multicast groups. Let $u_{ijkl} = 1$ if multicast group $i$ is served by the RIS at site $j$ with orientation $l$ and the BS at site $k$, and $u_{ijkl} = 0$ otherwise. We also define RIS location as a binary indicator $x_{jl}$. Let $x_{jl} = 1$ if a RIS is deployed at node $j$ with orientation $l$, and $x_{jl} = 0$ otherwise. By analogy, we define BS location as a binary indicator $y_k$. Specifically, $y_k = 1$ if a BS is deployed at site $k$, and $y_k = 0$ otherwise. We, therefore, have the following constraints:

$$u_{ijkl} \leq x_{jl}, i \in \mathcal{N}_{\text{group}}, j \in \mathcal{L}_{\text{RIS}}, k \in \mathcal{L}_{\text{BS}}, l \in \mathcal{L}_{\theta}, \tag{9}$$

$$u_{ijkl} \leq y_k, i \in \mathcal{N}_{\text{group}}, j \in \mathcal{L}_{\text{RIS}}, k \in \mathcal{L}_{\text{BS}}, l \in \mathcal{L}_{\theta}. \tag{10}$$

We then assume the constraints on the maximum number of RISs and BSs to be deployed:

$$1 \leq \sum_{j \in \mathcal{L}_{\text{RIS}}} \sum_{l \in \mathcal{L}_{\theta}} x_{jl} \leq N_{\text{RIS}}, \; 1 \leq \sum_{k \in \mathcal{L}_{\text{BS}}} y_k \leq N_{\text{BS}}. \tag{11}$$

Furthermore, a single orientation of the RIS can be utilized during the RIS deployment at any node $j$:

$$\sum_{l \in L_{\theta}} x_{jl} \leq 1, j = j_0, \tag{12}$$

where $j_0 \in \mathcal{L}_{\text{RIS}}$ is one of the possible sites where a RIS can be placed.

The optimal multi-RIS deployment problem in 5G NR/B5G cellular networks with multicast communications can be therefore modeled as follows:

$$\max \sum_{i \in \mathcal{N}_{\text{group}}} \sum_{j \in \mathcal{L}_{\text{RIS}}} \sum_{k \in \mathcal{L}_{\text{BS}}} \sum_{l \in \mathcal{L}_{\theta}} D_{ijkl} u_{ijkl}, \tag{13}$$
$$\text{s.t.}(9), (10), (11), (12).$$

We solve (13) using a *branch and bound algorithm*, which decomposes the problem into sub-problems. The algorithm provides an initial upper and lower bound of the solution and then proceeds to improve them by solving the discovered sub-problems until their difference is less than a fixed value or the elapsed time/number of iterations exceed a predefined threshold.

As the optimal multi-RIS deployment problem in B5G multicast systems represents a special case of the facility location problem, which has been proven to be NP-hard [20], we implement supervised ML algorithms to obtain the close-to-optimal solution of the problem in a reasonable time.

### B. Supervised Multiclass Classification ML Algorithms

Once the optimal multi-RIS deployment problem is solved, we can exploit the correlation between the ML algorithm inputs and the optimal solution that maximizes $D_{ijkl}$. From an ML perspective, we aim to find the corresponding $j$ and $l$ values for each multicast group $i$. To achieve this, we define the problem as a supervised ML multiclass classification problem [21], representing our training samples as $(X, y)$, where $X \in \{x_1, x_2, \ldots, x_F\}$ f and $y \in \{y_1, y_2, \ldots, y_C\}$ coresponds to $F$ features and $C$ classes, respectively. In this context, $C$ represents the problem space defined by all possible combinations of RIS locations and orientations $L_{\text{RIS}} \times L_{\theta}$. The goal of the training process is to obtain a learning model $\mathcal{H}$, such that $\mathcal{H}(X) = y$ for unseen samples of a testing dataset [21].

The features that best fit our multiclass classification problem space include the coordinates $XYZ_{i,k}^{worst}$ of the worst channel quality user $u_{i,k}^{worst}$ in the multicast group, the set of distances between $u_{i,k}^{worst}$ and the $L_{\text{RIS}}$ RIS locations, $d_{i,k}^{worst}$, as well as $x_{j,l}$ and $N_{\text{group}}$. Then, $X$ is defined as $\{XYZ_{i,k}^{worst}, d_{i,k}^{worst}, x_{j,l}, N_{\text{group}}\}$.

We generate a dataset of 20000 samples to train our ML models based on our optimal multi-RIS deployment solution. We use the Python library SMOTE (Synthetic Minority Oversampling Technique) [22] to oversample the minority classes and train the ML multiclass classification models with a balanced dataset. The training process of the ML algorithms includes data processing to avoid outliers, data normalization (Min-Max scaling method), a train/test split (**80%** and **20%** for the training and testing, respectively), grid-search and k-fold cross-validation (with $k = 10$). Finally, the algorithms are evaluated through specific error metrics such as classification accuracy, F1 score, precision, and recall [23].

To find the optimal learning model $\mathcal{H}$, we evaluate the performance of several scikit-learn natives multiclass classifiers and binary classifiers with One-vs-One (OVO) strategy and One-vs-Rest (OVR) [23]. After multiple iterations, the best performance is achieved with Extra-Trees Classifier (ETC) [24] used as a binary classifier on top of an OVR strategy, ETC-OVR.

## IV. Numerical Results

This section collects the numerical results on RIS deployment and orientation in multicast cellular networks through our optimal RIS deployment framework and supervised ML algorithms.

We consider a 50m $\times$ 50m UMi Street Canyon open area with a BS operating at 28 GHz and 30 UEs [15]. Since BS deployment is widely studied in the literature, we assume that the BS is in the middle of the area of interest and employs a linear antenna array with $\{128, 64, 32, 16, 8, 4, 2, 1\} \times 4$ antenna elements. Moreover, we adopt a fixed transmit power of 33 dBm. Then, we assume that the UEs are already split into multicast groups since multicast group formation is out of the scope of this paper. However, we note that our algorithms are compatible with any group formation strategy [25].

We assume that the channel state information (CSI) is known for both BS-UE and RIS-enhanced links [26], and each reflective element has a unit-gain reflection coefficient, i.e., $|\Gamma_q| = 1$, and signals reflected by different reflective elements arrive aligned in phase at the receiver [27]. RISs are composed of $4096$ reflective elements having a unit efficiency, $\epsilon_b = 1$, and a size equal to $\lambda/8$ [28]. Finally, we summarize the default simulation parameters in Table I.

We begin with the performance analysis of our optimal RIS deployment framework. We consider a 3D grid of $400$ possible RIS sites, as presented in Fig. 2. Moreover, once deployed, we assume that each RIS holds an LoS no-blockage condition towards both the BS and the UEs [27] and must adopt one of the following possible orientations: $[0; \pi]$, $[\pi/6; 7\pi/6]$, $[\pi/4; 5\pi/4]$, $[\pi/3; 4\pi/3]$, $[\pi/2; 3\pi/2]$, $[2\pi/3; 5\pi/3]$, $[3\pi/4; 7\pi/4]$, $[5\pi/6; 11\pi/6]$, $[\pi; 2\pi]$, $[-5\pi/6; \pi/6]$, $[-3\pi/4; \pi/4]$, $[-2\pi/3; \pi/3]$, $[-\pi/2; \pi2]$, $[-\pi/3; 2\pi3]$, $[-\pi/4; 3\pi/4]$, $[-\pi/6; 5\pi/6]$. As per [18], we assume that the optimal *vertical orientation* of RIS is always $\pi/2$, i.e., the RIS is deployed vertically to the BS. In this work, we determine the optimal *horizontal orientation* of RIS, which depends on the UEs' locations.

TABLE I
NUMERICAL SIMULATIONS DEFAULT PARAMETERS.

| Parameter | Value |
|---|---|
| Area of interest, $w_{\mathrm{SA}}$ x $l_{\mathrm{SA}}$ | 50 m x 50 m [15] |
| Number of UEs, $N_{\mathrm{UE}}$ | 30 |
| Number of multicast groups, $N_{\mathrm{group}}$ | 4 |
| Blockers density, $\lambda_{\mathrm{B}}$ | 20 bl/m$^2$ |
| BS operating frequency, $f_c$ | 28 GHz |
| Bandwidth, $W_{\mathrm{GHz}}$ | 1 GHz |
| Power spectral density of noise, $N_0$ | $10^{-\frac{174}{10}}$ W/Hz |
| Transmit power, $P_t$ | 1.9953 W |
| Number of reflective elements, $M_{\mathrm{SE}} \times N_{\mathrm{SE}}$ | 4096 |
| BS height, $h_{\mathrm{BS}}$ | 10 m [15] |
| UE height, $h_{\mathrm{UE}}$ | 1.5 m [15] |
| Blocker radius, $r_{\mathrm{B}}$ | 0.4 m |
| Blocker height, $h_{\mathrm{B}}$ | 1.7 m [15] |
| Number of BSs, $N_{\mathrm{BS}}$ | 1 |
| Number of employable RISs, $N_{\mathrm{RIS}}$ | 2 - 6 |
| Propagation coefficient, $\zeta$ | 2.1 - 3.19 [15] |
| Blockage coefficient, $\beta$ | 32.4 - 47.4 [15], [16] |
| BS antenna array | $\{128, 64, 32, 16, 8, 4, 2, 1\} \times 4$ |
| Packet Size | 1 Gbit |

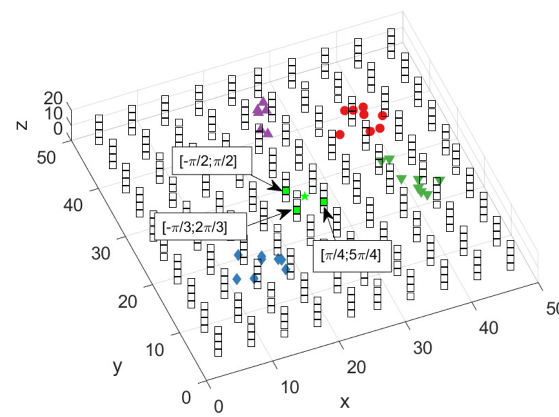


Fig. 2. Example of optimal multi-RIS deployment and orientation in multicast systems. Red circles, blue rhombus, green, and purple triangles are multicast groups, white squares are possible RIS sites, green squares are optimal RIS sites, and the green star is the BS.

### A. Multicast-aided RIS Assessment

To evaluate the benefits of RIS-enhanced links for multicast communications, we compare our RIS-aided solution with two benchmarks: (i) **Multicast without RIS** and (ii) **Unicast**. In the former case, the BS communicates with the users through multicast communications employing *Conventional Multicast Scheme* (CMS), wherein the data rate of a multicast group is bounded by the user with the worst channel conditions. In the latter one, sequential unicast BS-UE transmissions are considered. Generally, the use of multicast service delivery with CMS results in more efficient resource utilization compared to unicast communications. This advantage is particularly noticeable when multicast users have similar and good channel

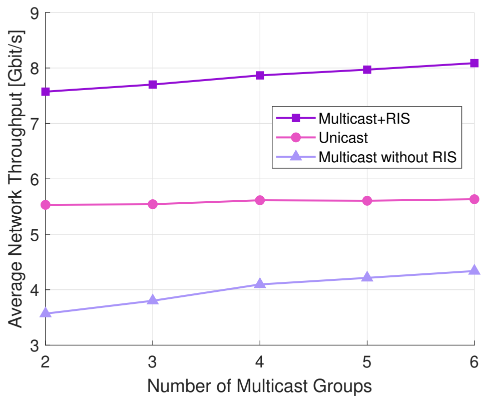


Fig. 3. Average network throughput as function of number of multicast groups.

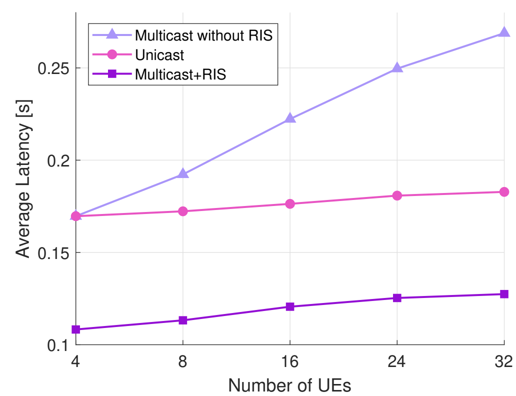


Fig. 4. Average latency as function of the number of UEs with 4 multicast groups.

conditions. In our numerical results, we extract users' channel conditions by employing (4) and (5). As shown in Fig. 3, unicast communications have higher network throughput than multicast communications due to poor channel conditions for UEs in the multicast group affecting performance when employing CMS. However, using RIS in multicast communications can improve UEs channel conditions for UEs and increase throughput by an average of nearly $30\%$ compared to unicast.

One may also see that the network throughput of multicasting, both with and without RIS, improves when the number of multicast groups grows. This behavior can be explained by the fact that we consider 30 UEs, meaning that the increase in the number of groups leads to a lower number of UEs per group, which might be critical in directional multicasting.

Determining the optimal horizontal orientation of a RIS is crucial for supporting cellular communications, as a RIS can only provide coverage to the half-space in front of it. This is especially important for multicast transmissions, as a RIS cannot support a multicast group if any UE in the group is not in its coverage area. Our simulations have shown that the most effective horizontal orientations are those that provide wide coverage of UEs, increasing the probability of simultaneously reaching all multicast users in a group: $[0;\pi]$, $[\pi/2;3\pi/2]$, $[\pi;2\pi]$, $[-\pi/2;\pi/2]$.

Moreover, enhancing multicast communications through RISs becomes even more vital in crowded areas to satisfy the stringent requirements of the most recent multimedia services. As shown in Fig. 4, multicast and unicast communications performance are equal for four network users since having a user for each multicast group corresponds to unicast transmissions. Then, multicast communications latency deteriorates as the number of UEs increases due to the higher probability of having users with shoddy channel conditions in a multicast group. In this case, RIS-aided multicast communication experiences a degradation in performance as the number of UEs increases (see the inclination of "Multicast without RIS" compared to "Multicast+RIS").

TABLE II
MULTICLASS CLASSIFICATION LEARNING MODELS EVALUATION.

| Algorithm | Model | Accuracy | Precision | Recall | F1 |
|---|---|---|---|---|---|
| ML-RPM | $\mathcal{H}_{C=20}$ (%) | 80.30 | 80.45 | 80.20 | 80.00 |
| sML-RPM | $\mathcal{H}^{1,2}_{C=10}$ (%) | 88.00 | 88.00 | 88.90 | 87.77 |
| sML-RPM | $\mathcal{H}^{3,4}_{C=10}$ (%) | 88.38 | 88.70 | 88.40 | 88.29 |

## B. ML Algorithms Assessment

The dataset used for training the ML models was created subject to the above assumptions. After data processing, we identified that for the **99.9%** of the samples, only four positions were selected from the total of 400 available positions. The $(x, y)$ coordinates (in meters) of such four RIS, regarding Fig. 2, are $(23, 23)_1$, $(23, 27)_2$, $(27, 23)_3$ and $(27, 27)_4$, around the BS located at $(25, 25)$. From the ML perspective, the remaining samples for other RIS positions, or not RIS (i.e., direct BS-multicast group link), were treated as outliers. Then for our multiclass classification problem, we consider four RIS positions with five possible orientations for a total of 20 potential classes ($C = 20$) for each dataset sample.

We identify our baseline multiclass classification suboptimal ML RIS Placement for Multicasting solution as ML-RPM for the problem space of $C = 20$, with a learning model $\mathcal{H}_{C=20}$ based on ETC-OVR. Moreover, regarding the identified symmetry of the classification problem space defined by the four RIS positions around the BS, we consider an alternative solution, training two independent ETC-OVR algorithms. The first mode, $\mathcal{H}^{1,2}_{C=10}$ is for the samples corresponding to the RIS positions $(23, 23)_1$, $(23, 27)_2$ with $C = 10$, and the second one, $\mathcal{H}^{3,4}_{C=10}$ is for the samples with the RIS positions $(27, 23)_3$ and $(27, 27)_4$ with $C = 10$. The algorithm executes both ML learning models for an unseen multicast group sample and selects the solution that maximizes (8). We identify this algorithm as sML-RPM. Table II summarizes the multiclass classification assessment of the trained ML models.

As shown in Table II, the trained models for $C = 10$ achieve higher performance. The models learn the patterns from a reduced problem space avoiding induced biases by the symmetry of the four RIS locations and available orientations. The penalty of sML-RPM is the increased computational complexity since two ML algorithms must be run to select the RIS position and orientation. The ML models, especially the sML-RPM algorithm, can classify the dataset samples with relatively good accuracy, precision, recall (sensitivity), and F1 score and provide near-optimal RIS placement and orientation results.

## V. Conclusion

In mmWave multicast communications, RISs will play a crucial role in enhancing the channel conditions of underperforming users in multicast groups, thereby improving overall performance. Despite RISs potential benefits, much remains to be explored regarding RIS deployment strategies that can enable their practical utilization in real-world scenarios. In this work, we formulated the RIS deployment and orientation problem in 5G/B5G cellular networks with directional multicast communications as a facility location problem. We first solved the problem using a branch and bound algorithm and evaluated the impact of RISs on multicast communications, demonstrating the substantial benefits of RIS employment for multicasting as the number of users and multicast groups vary. We then utilized the resulting dataset from the optimal solution for training ML multiclass classification algorithms.

The proposals of this study can be utilized as a valuable tool for optimizing and analyzing RIS deployment in various scenarios. As a potential area of investigation for future research, it will be essential to explore the impact of user mobility and multi-reflection multi-RIS paths on RIS deployment to gain a deeper understanding of practical RIS installation.

## Acknowledgment

The authors gratefully acknowledge funding from European Union's Horizon 2020 Research and Innovation programme under the Marie Skłodowska Curie grant agreement No. 813278 (A-WEAR, http://www.a-wear.eu/).

## References

[1] D. Mi, J. Eyles, T. Jokela, S. Petersen, R. Odarchenko, E. Öztürk, D.-K. Chau, T. Tran, R. Turnbull, H. Kokkinen, *et al.*, "Demonstrating Immersive Media Delivery on 5G Broadcast and Multicast Testing Networks," *IEEE Transactions on Broadcasting*, vol. 66, no. 2, pp. 555–570, 2020.

[2] V. K. Shrivastava, S. Baek, and Y. Baek, "5G Evolution for Multicast and Broadcast Services in 3GPP Release 17," *IEEE Communications Standards Magazine*, vol. 6, no. 3, pp. 70–76, 2022.

[3] G. Araniti, P. Scopelliti, G.-M. Muntean, and A. Iera, "A hybrid unicast-multicast network selection for video deliveries in dense heterogeneous network environments," *IEEE Transactions on Broadcasting*, vol. 65, no. 1, pp. 83–93, 2018.

[4] G. Araniti, M. Condoluci, M. Cotronei, A. Iera, and A. Molinaro, "A solution to the multicast subgroup formation problem in lte systems," *IEEE Wireless Communications Letters*, vol. 4, no. 2, pp. 149–152, 2015.

[5] A. de la Fuente, G. Interdonato, and G. Araniti, "User Subgrouping and Power Control for Multicast Massive MIMO Over Spatially Correlated Channels," *IEEE Transactions. on Broadcasting*, vol. 68, no. 4, pp. 834–847, 2022.

[6] N. Chukhno, O. Chukhno, S. Pizzi, A. Molinaro, A. Iera, and G. Araniti, "Efficient Management of Multicast Traffic in Directional mmWave Networks," *IEEE Transactions on Broadcasting*, vol. 67, no. 3, pp. 593–605, 2021.

[7] L. Jiao, P. Wang, A. Alipour-Fanid, H. Zeng, and K. Zeng, "Enabling Efficient Blockage-Aware Handover in RIS-Assisted mmWave Cellular Networks," *IEEE Transactions on Wireless Communications*, vol. 21, no. 4, pp. 2243–2257, 2021.

[8] Q. Wu and R. Zhang, "Towards Smart and Reconfigurable Environment: Intelligent Reflecting Surface Aided Wireless Network," *IEEE Communications Magazine*, vol. 58, no. 1, pp. 106–112, 2019.

[9] A. Orsino, G. Araniti, A. Molinaro, and A. Iera, "Effective rat selection approach for 5g dense wireless networks," in *2015 IEEE 81st vehicular technology conference (VTC Spring)*, pp. 1–5, IEEE, 2015.

[10] F. Qi, Q. Liu, W. Li, P. Yu, and X. Qiu, "Enhanced 5G Mobile Broadcasting Service With Shape-Adaptive RIS," *IEEE Transactions on Broadcasting*, 2022.

[11] L. Du, S. Shao, G. Yang, J. Ma, Q. Liang, and Y. Tang, "Capacity Characterization for Reconfigurable Intelligent Surfaces Assisted Multiple-Antenna Multicast," *IEEE Transactions on Wireless Communications*, vol. 20, no. 10, pp. 6940–6953, 2021.

[12] Y. Li, C. Yin, T. Do-Duy, A. Masaracchia, and T. Q. Duong, "Aerial Reconfigurable Intelligent Surface-Enabled URLLC UAV Systems," *IEEE Access*, vol. 9, pp. 140248–140257, 2021.

[13] Q. Bie, Y. Liu, Y. Wang, X. Zhao, and X. Y. Zhang, "Deployment Optimization of Reconfigurable Intelligent Surface for Relay Systems," *IEEE Transactions on Green Communications and Networking*, vol. 6, no. 1, pp. 221–233, 2022.

[14] O. Chukhno, N. Chukhno, O. Galinina, Y. Gaidamaka, S. Andreev, and K. Samouylov, "Analysis of 3D Deafness Effects in Highly Directional mmWave Communications," in *2019 IEEE Global Communications Conference (GLOBECOM)*, pp. 1–6, IEEE, 2019.

[15] "Study on Channel Model for Frequencies from 0.5 to 100 GHz (Release 14)," tech. rep., 3GPP TR 38.901 V14.1.1, July 2017.

[16] V. Raghavan, V. Podshivalov, J. Hulten, M. A. Tassoudji, A. Sampath, O. H. Koymen, and J. Li, "Spatio-Temporal Impact of Hand and Body Blockage for Millimeter-Wave User Equipment Design at 28 GHz," *IEEE Communications Magazine*, vol. 56, no. 12, pp. 46–52, 2018.

[17] M. Gapeyenko, A. Samuylov, M. Gerasimenko, D. Moltchanov, S. Singh, E. Aryafar, S.-p. Yeh, N. Himayat, S. Andreev, and Y. Koucheryavy, "Analysis of Human-Body Blockage in Urban Millimeter-Wave Cellular Communications," in *2016 IEEE International Conference on Communications (ICC)*, pp. 1–7, IEEE, 2016.

[18] S. Zeng, H. Zhang, B. Di, Z. Han, and L. Song, "Reconfigurable Intelligent Surface (RIS) Assisted Wireless Coverage Extension: RIS Orientation and Location Optimization," *IEEE Communications Letters*, vol. 25, no. 1, pp. 269–273, 2020.

[19] S. W. Ellingson, "Path loss in Reconfigurable Intelligent Surface-enabled Channels," in *2021 IEEE 32nd Annual International Symposium on Personal, Indoor and Mobile Radio Communications (PIMRC)*, pp. 829–835, IEEE, 2021.

[20] H. A. Eiselt and V. Marianov, *Foundations of Location Analysis*, vol. 155. Springer Science & Business Media, 2011.

[21] M. Aly, "Survey on Multiclass Classification Methods," *Neural Netw*, vol. 19, no. 1-9, p. 2, 2005.

[22] N. V. Chawla, K. W. Bowyer, L. O. Hall, and W. P. Kegelmeyer, "SMOTE: Synthetic Minority Over-Sampling Technique," *Journal of artificial intelligence research*, vol. 16, pp. 321–357, 2002.

[23] A. Géron, *Hands-On Machine Learning with Scikit-Learn, Keras, and TensorFlow*. " O'Reilly Media, Inc.", 2022.

[24] P. Geurts, D. Ernst, and L. Wehenkel, "Extremely Randomized Trees," *Machine learning*, vol. 63, pp. 3–42, 2006.

[25] N. Chukhno, O. Chukhno, S. Pizzi, A. Molinaro, A. Iera, and G. Araniti, "Unsupervised Learning for D2D-Assisted Multicast Scheduling in mmWave Networks," in *2021 IEEE International Symposium on Broadband Multimedia Systems and Broadcasting (BMSB)*, pp. 1–6, IEEE, 2021.

[26] X. Tian, N. Gonzalez-Prelcic, and R. W. Heath Jr, "Optimizing the Deployment of Reconfigurable Intelligent Surfaces in MmWave Vehicular Systems," *arXiv preprint arXiv:2205.15520*, 2022.

[27] I. Yildirim, A. Uyrus, and E. Basar, "Modeling and Analysis of Reconfigurable Intelligent Surfaces for Indoor and Outdoor Applications in Future Wireless Networks," *IEEE Transactions on Communications*, vol. 69, no. 2, pp. 1290–1301, 2020.

[28] M. Di Renzo, A. Ahmed, A. Zappone, V. Galdi, G. Gradoni, M. Moccia, and G. Castaldi, "Digital Reconfigurable Intelligent Surfaces: On the Impact of Realistic Reradiation Models," *arXiv preprint arXiv:2205.09799*, 2022.